

Asymmetric mass ratios for bright double neutron-star mergers

<https://doi.org/10.1038/s41586-020-2439-x>

Received: 19 December 2019

Accepted: 14 April 2020

Published online: 8 July 2020

 Check for updates

R. D. Ferdman^{1✉}, P. C. C. Freire², B. B. P. Perera³, N. Pol^{4,5}, F. Camilo⁶, S. Chatterjee^{7,8}, J. M. Cordes^{7,8}, F. Crawford⁹, J. W. T. Hessels^{10,11}, V. M. Kaspi^{12,13}, M. A. McLaughlin^{4,5}, E. Parent^{12,13}, I. H. Stairs¹⁴ & J. van Leeuwen¹¹

The discovery of a radioactively powered kilonova associated with the binary neutron-star merger GW170817 remains the only confirmed electromagnetic counterpart to a gravitational-wave event^{1,2}. Observations of the late-time electromagnetic emission, however, do not agree with the expectations from standard neutron-star merger models. Although the large measured ejecta mass^{3,4} could be explained by a progenitor system that is asymmetric in terms of the stellar component masses (that is, with a mass ratio q of 0.7 to 0.8)⁵, the known Galactic population of merging double neutron-star systems (that is, those that will coalesce within billions of years or less) has until now consisted only of nearly equal-mass ($q > 0.9$) binaries⁶. The pulsar PSR J1913+1102 is a double system in a five-hour, low-eccentricity (0.09) orbit, with an orbital separation of 1.8 solar radii⁷, and the two neutron stars are predicted to coalesce in 470_{-11}^{+12} million years owing to gravitational-wave emission. Here we report that the masses of the pulsar and the companion neutron star, as measured by a dedicated pulsar timing campaign, are 1.62 ± 0.03 and 1.27 ± 0.03 solar masses, respectively. With a measured mass ratio of $q = 0.78 \pm 0.03$, this is the most asymmetric merging system reported so far. On the basis of this detection, our population synthesis analysis implies that such asymmetric binaries represent between 2 and 30 per cent (90 per cent confidence) of the total population of merging binaries. The coalescence of a member of this population offers a possible explanation for the anomalous properties of GW170817, including the observed kilonova emission from that event.

Since its discovery⁷ in 2012, we have been regularly monitoring the double neutron star (DNS) PSR J1913+1102 with the Arecibo radio telescope. Our observations have used the Mock Spectrometer and the Puerto Rico Ultimate Pulsar Processing Instrument (PUPPI) to coherently remove dispersive smearing from the pulsar signal, caused by the interstellar free-electron plasma along the line of sight to the pulsar. We analysed data from this pulsar using standard pulse timing techniques (see Methods).

With a spin period of 27 ms, PSR J1913+1102 was probably the first-formed neutron star in this binary system; it subsequently gained angular momentum via accretion of matter from the progenitor to the second neutron star⁷. The timing of the pulsar has allowed a precise measurement of the rate of advance of the periastron, which is $\dot{\omega} = (5.6501 \pm 0.0007) \text{ yr}^{-1}$. In addition, we have now determined two more post-Keplerian parameters: the first is the Einstein delay ($\gamma = 0.471 \pm 0.015$ ms), which describes the effect of gravitational

redshift and relativistic time dilation due to the varying orbital velocity and proximity of the neutron stars to one another during their orbits. The second is the decay of the orbital period caused by the emission of gravitational waves ($\dot{P}_b = (-4.8 \pm 0.3) \times 10^{-13} \text{ s s}^{-1}$).

In Fig. 1, we show the general-relativistic mass constraints corresponding to each measured post-Keplerian parameter. From $\dot{\omega}$, the total system mass is $(2.8887 \pm 0.0006)M_{\odot}$ (M_{\odot} , solar mass), making PSR J1913+1102 the most massive among known DNS systems (by a 2% margin). By combining $\dot{\omega}$ and γ , we obtain the individual neutron-star masses $m_p = (1.62 \pm 0.03)M_{\odot}$ and $m_c = (1.27 \pm 0.03)M_{\odot}$ (unless otherwise stated, uncertainties denote 68% confidence) for the pulsar and the companion, respectively, which give a mass ratio of $q = m_c/m_p = 0.78 \pm 0.03$. The observed \dot{P}_b is consistent with the general relativity prediction for these neutron-star masses; apart from confirming them, this effect provides a unique test of alternative gravitational theories that will be reported elsewhere (P.C.C.F. et al., manuscript in

¹Faculty of Science, University of East Anglia, Norwich, UK. ²Max-Planck-Institut für Radioastronomie, Bonn, Germany. ³Arecibo Observatory, Arecibo, Puerto Rico. ⁴Department of Physics and Astronomy, West Virginia University, Morgantown, WV, USA. ⁵Center for Gravitational Waves and Cosmology, West Virginia University, Morgantown, WV, USA. ⁶South African Radio Astronomy Observatory, Cape Town, South Africa. ⁷Cornell Center for Astrophysics and Planetary Science, Cornell University, Ithaca, NY, USA. ⁸Department of Astronomy, Cornell University, Ithaca, NY, USA. ⁹Department of Physics and Astronomy, Franklin and Marshall College, Lancaster, PA, USA. ¹⁰Anton Pannekoek Institute for Astronomy, University of Amsterdam, Amsterdam, The Netherlands. ¹¹ASTRON, Netherlands Institute for Radio Astronomy, Dwingeloo, The Netherlands. ¹²Department of Physics, McGill University, Montreal, Quebec, Canada. ¹³McGill Space Institute, McGill University, Montreal, Quebec, Canada. ¹⁴Department of Physics and Astronomy, University of British Columbia, Vancouver, British Columbia, Canada.

✉e-mail: r.ferdman@uea.ac.uk

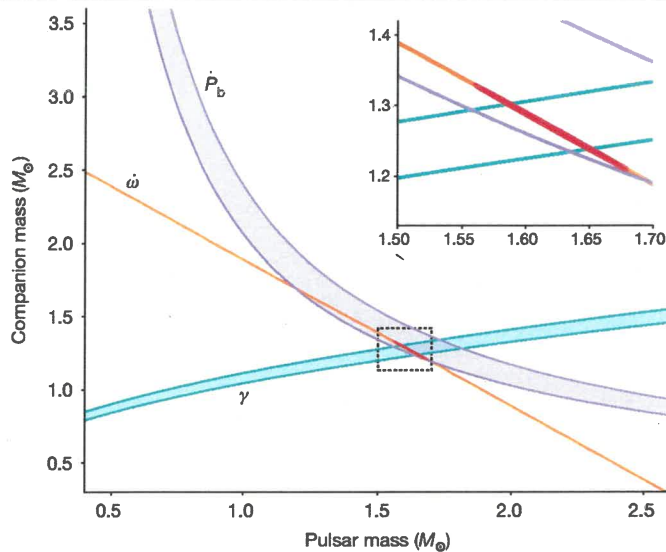


Fig. 1 | Pulsar mass–companion mass diagram for the PSR J1913+1102 system. Shaded regions bounded by solid curves represent 1σ mass constraints from each measured post-Keplerian parameter, derived in the context of general relativity. These are: the orbital precession rate ($\dot{\omega}$), the time dilation/gravitational redshift (γ) and the rate of orbital decay (\dot{P}_b). The inset shows a zoom-in of the dotted square region in the main plot, with the 3σ confidence region for the mass measurements shaded in red. The two most precisely measured parameters allow us to determine the individual masses of this system. Each additional post-Keplerian parameter measurement provides an independent consistency test of the predictions of general relativity.

preparation). Table 1 summarizes the best-fit model parameters for the PSR J1913+1102 system.

PSR J1913+1102 is part of a population of several very compact DNS binary systems with moderate orbital eccentricities (≤ 0.2) and low proper motions (for example, PSRs J0737–3039A/B⁸, J1756–2251⁹ and J1946+2052¹⁰). These imply an evolutionary path in which the second-formed neutron star is born as a result of an envelope-stripped

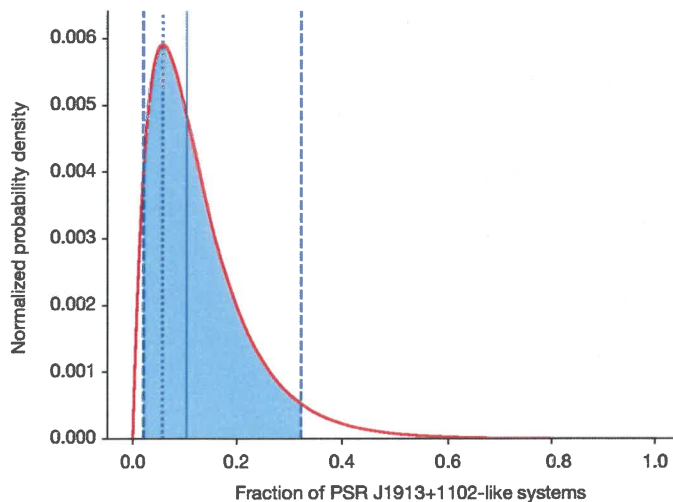


Fig. 2 | Probability density of the population of PSR J1913+1102-like DNS systems in the Galaxy, as a fraction of the total number of DNSs that will merge within a Hubble time. We find this fraction to be $0.11^{+0.21}_{-0.09}$, where the uncertainty represents the 90% confidence interval (vertical dashed lines). The quoted value is the median of the distribution, shown on the plot as a solid vertical line, and the peak value of 0.06 is represented by a dotted vertical line. This implies that roughly 1 in 10 merging DNS systems are likely to have asymmetric component masses.

Table 1 | Measured and derived parameters for PSR J1913+1102

Parameter name	Value
Reference epoch (MJD)	57,504.0
Observing time span (MJD)	56,072–58,747
Number of arrival time measurements	2,541
Solar System ephemeris used	DE436
Root-mean-square timing residual	56 μ s
Reduced χ^2 of timing fit	1.01
Right ascension, α (J2000)	19 h 13 min 29.05365(9) s
Declination, δ (J2000)	1 $^{\circ}$ 02' 05.7045(22) $''$
Proper motion in α	–3.0(5) mas yr $^{-1}$
Proper motion in δ	–8.7(1.0) mas yr $^{-1}$
Pulsar spin period, P	27.2850068680286(19) ms
Spin period derivative, \dot{P}	$1.5672(7) \times 10^{-19}$ s s $^{-1}$
Dispersion measure, DM	339.026(3) pc cm $^{-3}$
Orbital period, P_b	0.2062523345(2) d
Projected semi-major axis of the pulsar's orbit, x	1.754635(5) light s
Orbital eccentricity, e	0.089531(2)
Longitude of periastron, ω	283.7898(19) $^{\circ}$
Epoch of periastron passage, T_0 (MJD)	57,504.5314530(10)
Total system mass, M	2.8887(6) M_{\odot}
Companion mass, M_c	1.27(3) M_{\odot}
Rate of periastron advance ^a , $\dot{\omega}$	5.6501(7) $^{\circ}$ yr $^{-1}$
Einstein delay ^a , γ	0.000471(15) s
Orbital period decay rate ^a , \dot{P}_b	$-4.8(3) \times 10^{-13}$ s s $^{-1}$
Pulsar mass, M_p	1.62(3)
Mass ratio, q	0.78(3)
Orbital inclination angle, i	55.3 $^{\circ}$
Dispersion-derived distance ^b , d	7.14 kpc
Two-dimensional systemic peculiar velocity ^c , v_{LSR}	100(70) km s $^{-1}$
Surface magnetic flux density at the poles ^d , B_0	2.1×10^9 G
Characteristic age ^d , τ_c	2.8 Gyr
Time to coalescence, T_c	470^{+12}_{-11} Myr

Values in parentheses represent the 1σ (68% confidence) uncertainty on the last quoted digit. Unless otherwise noted, measured parameters were determined using the DDGR timing model^{43,44}, which assumes general relativity to be the correct theory of gravity. MJD, modified Julian date.

^aPost-Keplerian orbital parameters were measured using the model-independent Damour and Deruelle timing model^{43–45}.

^bDistance is derived using a model of the Galactic ionized electron density⁴⁶, with estimated uncertainty of 20%.

^cVelocity is with respect to the local standard of rest, and thus peculiar to the binary system.

^dThe surface magnetic field and characteristic age are derived from the pulsar spin period and its derivative⁴⁷.

helium star progenitor having undergone a supernova with very little mass loss and low natal kick^{6,11}, owing to either a rapid iron core collapse event or electron capture onto an oxygen–neon–magnesium core^{12–14}. Either of these scenarios lead to a low-mass ($\leq 1.3M_{\odot}$) neutron star⁷, which is confirmed by our measurements. Furthermore, we estimate the tangential component of the peculiar velocity of the system to be 100 ± 70 km s $^{-1}$ (95% confidence); although the uncertainty is still large, this hints at a relatively low kick velocity arising from the second supernova compared to the overall pulsar population.

The PSR J1913+1102 mass ratio makes it the most asymmetric among the known DNS binaries that are expected to merge within a Hubble time, which otherwise have $q \geq 0.9$. Considering all known DNS systems,

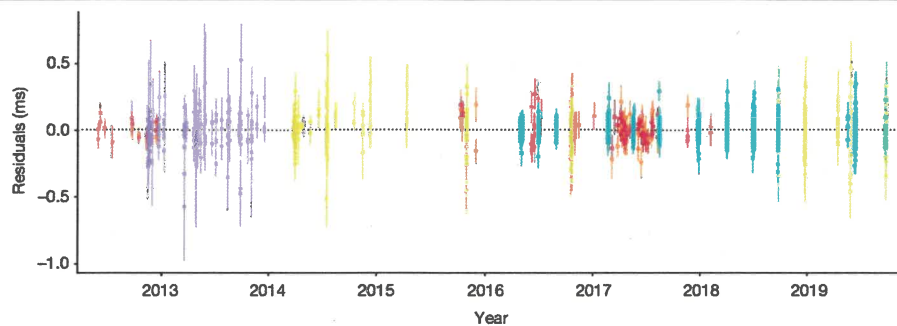


Fig. 3 | Post-fit timing residuals for PSR J1913+1102. These are obtained after including all best-fit parameters in the Damour and Deruelle General Relativity (DDGR) model^{43,44} ephemeris for this pulsar. Each contributing instrument is represented by different colours: Mock spectrometer centred at 1,300 MHz (orange) and at 1,450 MHz (red); PUPPI centred at 1,400 MHz in incoherent mode (purple); PUPPI centred at 1,400 MHz in coherent-fold mode (yellow);

and PUPPI centred at 2,350 MHz in coherent-fold mode (cyan). The latter provided a substantial improvement in data quality, as evidenced by the reduction in the weighted root-mean-square timing residuals to 48 μ s, down from 72 μ s at 1,400 MHz in coherent mode. The error bars shown reflect the 1 σ (68%) uncertainties of each data point.

the only one having a similar mass asymmetry is PSR J0453+1559¹⁵, with $q = 0.753 \pm 0.005$; however, its orbital period of 4.07 days implies a coalescence time about 100 times greater than the age of the Universe. By contrast, PSR J1913+1102 has an expected time to coalescence of 470_{-11}^{+12} Myr, which we determined from the orbital decay rate and other measured orbital elements.

There are currently nine confirmed compact DNS binaries that are predicted to merge within a Hubble time, for which precise neutron-star mass measurements have been made⁶. We performed a population synthesis analysis for these DNS systems, including PSR J1913+1102, using their individual properties and known masses (see also Methods). We found that PSR J1913+1102-like binaries represent 11_{-9}^{+21} % of merging DNS systems (Figs. 2, 3), where the quoted value is the median and the errors represent the 90% confidence intervals. This therefore establishes the existence of a population of asymmetric DNS systems that is sizable enough to potentially lead to the discovery of several corresponding merger events by ground-based gravitational-wave observatories such as LIGO/Virgo. As such, the discovery of PSR J1913+1102 provides evidence for the need to account for asymmetric coalescing DNS binaries—approximately one-tenth of events—in interpreting merger scenarios and the underpinning physics.

Observations of the electromagnetic counterparts to the GW170817 event have largely been related to a relatively large amount of ejecta due to the preceding DNS merger, with masses of the order of $0.05M_{\odot}$ (refs. 4,16). This is at odds with standard models of DNS coalescence, which typically predict smaller ejecta mass by at least a factor of 5, primarily on the basis of the assumption of equal-mass (or near-equal-mass) progenitor DNS binary systems^{5,17,18}. Until recently, this has been a reasonable assumption given the known DNS population⁶. It is plausible that the anomalously massive ejecta inferred from the observed late-time emission in the case of GW170817 may be explained with an equal-mass system, particularly if one includes a secular component to the ejecta^{19–21}. The merger may also be explained by the invocation of various models to describe the observations. These include an off-axis jet from a short γ -ray burst^{22,23}; a mildly relativistic wide-angle outflow that interacts with the dynamic ejecta^{24,25}; a hyper-massive neutron-star remnant of the merger acting as a spin-down energy source^{26,27}; and a hierarchical triple system in which a disk is formed from a Roche lobe-filling outer star²⁸.

By contrast, numerical simulations have shown that high-asymmetry ($0.65 \leq q \leq 0.85$) systems will naturally produce larger tidal distortions during the merger phase and result in larger-mass, and therefore brighter, disks than those of roughly equal-mass systems^{18,29–31}. The resulting tidal effects consistently produce sufficient neutron-rich ejecta to power a kilonova and result in an enhancement of r-process material³². A sufficiently

unequal-mass binary that will merge within a Hubble time may therefore be responsible for events such as GW170817, particularly in the slow, $-0.04M_{\odot}$ red component seen in the latter⁴. A substantial population of asymmetric DNSs such as PSR J1913+1102 would therefore lead to an enhanced detection rate of bright kilonovae. The electromagnetic counterparts to such events are therefore particularly important for understanding the Galactic heavy-element abundance^{16,33,34}.

Enhanced pre-coalescence tidal distortions due to asymmetric mergers may also allow certain neutron-star equation-of-state models to be ruled out through study of the gravitational-wave waveform^{21,35–38}. Additionally, gravitational waves from merging DNSs have recently been used as distance indicators (so-called ‘standard sirens’), enabling an independent probe of the Hubble constant, H_0 , when combined with radial-velocity measurements of the electromagnetic counterparts³⁹. Future asymmetric DNS mergers with similar electromagnetic counterparts to those of GW170817 would lead to a considerably more precise determination of H_0 —about 15 suitable detections would provide a $\sim 2\%$ measurement⁴⁰—and potentially provide the means by which to resolve the disagreement between H_0 as measured from the cosmic microwave background⁴¹ and through local Universe analysis methods⁴².

Online content

Any methods, additional references, Nature Research reporting summaries, source data, extended data, supplementary information, acknowledgements, peer review information; details of author contributions and competing interests; and statements of data and code availability are available at <https://doi.org/10.1038/s41586-020-2439-x>.

- Abbott, B. et al. GW170817: observation of gravitational waves from a binary neutron star inspiral. *Phys. Rev. Lett.* **119**, 161101 (2017).
- Abbott, B. P. et al. Multi-messenger observations of a binary neutron star merger. *Astrophys. J. Lett.* **848**, 12 (2017).
- Abbott, B. P. et al. Estimating the contribution of dynamical ejecta in the kilonova associated with GW170817. *Astrophys. J. Lett.* **850**, 39 (2017).
- Cowperthwaite, P. S. et al. The electromagnetic counterpart of the binary neutron star merger LIGO/Virgo GW170817. II. UV, optical, and near-infrared light curves and comparison to kilonova models. *Astrophys. J. Lett.* **848**, 17 (2017).
- Pankow, C. On GW170817 and the Galactic binary neutron star population. *Astrophys. J.* **866**, 60 (2018).
- Tauris, T. M. et al. Formation of double neutron star systems. *Astrophys. J.* **846**, 170 (2017).
- Lazarus, P. et al. Einstein@Home discovery of a double neutron star binary in the PALFA survey. *Astrophys. J.* **831**, 150 (2016).
- Kramer, M. et al. Tests of general relativity from timing the double pulsar. *Science* **314**, 97–102 (2006).
- Ferdman, R. D. et al. PSR J1756–2251: a pulsar with a low-mass neutron star companion. *Mon. Not. R. Astron. Soc.* **443**, 2183–2196 (2014).
- Stovall, K. et al. PALFA discovery of a highly relativistic double neutron star binary. *Astrophys. J. Lett.* **854**, 22 (2018).

11. Tauris, T. M. et al. Ultra-stripped type Ic supernovae from close binary evolution. *Astrophys. J. Lett.* **778**, 23 (2013).
12. Miyaji, S., Nomoto, K., Yokoi, K. & Sugimoto, D. Supernova triggered by electron captures. *Publ. Astron. Soc. Jpn.* **32**, 303–329 (1980).
13. Nomoto, K. Evolution of 8–10 solar mass stars toward electron capture supernovae. I – formation of electron-degenerate O + NE + MG cores. *Astrophys. J.* **277**, 791–805 (1984).
14. Podsiadlowski, P. et al. The double pulsar J0737–3039: testing the neutron star equation of state. *Mon. Not. R. Astron. Soc.* **361**, 1243–1249 (2005).
15. Martinez, J. G. et al. Pulsar J0453+1559: a double neutron star system with a large mass asymmetry. *Astrophys. J.* **812**, 143 (2015).
16. Kasen, D., Metzger, B., Barnes, J., Quataert, E. & Ramirez-Ruiz, E. Origin of the heavy elements in binary neutron-star mergers from a gravitational-wave event. *Nature* **551**, 80–84 (2017).
17. Hotokezaka, K. et al. Mass ejection from the merger of binary neutron stars. *Phys. Rev. D* **87**, 024001 (2013).
18. Radice, D. & Dai, L. Multimessenger parameter estimation of GW170817. *Eur. Phys. J. A* **55**, 50 (2019).
19. Siegel, D. M. & Metzger, B. D. Three-dimensional GRMHD simulations of neutrino-cooled accretion disks from neutron star mergers. *Astrophys. J.* **858**, 52 (2018).
20. Fernández, R., Tchekhovskoy, A., Quataert, E., Foucart, F. & Kasen, D. Long-term GRMHD simulations of neutron star merger accretion discs: implications for electromagnetic counterparts. *Mon. Not. R. Astron. Soc.* **482**, 3373–3393 (2018).
21. Radice, D. et al. Binary neutron star mergers: mass ejection, electromagnetic counterparts and nucleosynthesis. *Astrophys. J.* **869**, 130 (2018).
22. Troja, E. et al. The X-ray counterpart to the gravitational-wave event GW170817. *Nature* **551**, 71–74 (2017).
23. Haggard, D. et al. A deep Chandra X-ray study of neutron star coalescence GW170817. *Astrophys. J.* **848**, L25 (2017).
24. Mooley, K. P. et al. A mildly relativistic wide-angle outflow in the neutron-star merger event GW170817. *Nature* **554**, 207–210 (2018).
25. Piro, A. L. & Kollmeier, J. A. Evidence for cocoon emission from the early light curve of SSS17a. *Astrophys. J.* **855**, 103 (2018).
26. Metzger, B. D., Thompson, T. A. & Quataert, E. A magnetar origin for the kilonova ejecta in GW170817. *Astrophys. J.* **856**, 101 (2018).
27. Li, S.-Z., Liu, L.-D., Yu, Y.-W. & Zhang, B. What powered the optical transient AT2017gfo associated with GW170817? *Astrophys. J. Lett.* **861**, 12 (2018).
28. Chang, P. & Murray, N. GW170817: A neutron star merger in a mass-transferring triple system. *Mon. Not. R. Astron. Soc. Lett.* **474**, 12–16 (2018).
29. Shibata, M. & Taniguchi, K. Merger of binary neutron stars to a black hole: disk mass, short gamma-ray bursts, and quasinormal mode ringing. *Phys. Rev. D* **73**, 064027 (2006).
30. Rezzolla, L., Baiotti, L., Giacomazzo, B., Link, D. & Font, J. A. Accurate evolutions of unequal-mass neutron-star binaries: properties of the torus and short GRB engines. *Class. Quantum Gravity* **27**, 114105 (2010).
31. Dietrich, T. & Ujevic, M. Modeling dynamical ejecta from binary neutron star mergers and implications for electromagnetic counterparts. *Class. Quantum Gravity* **34**, 105014 (2017).
32. Lehner, L. et al. Unequal mass binary neutron star mergers and multimessenger signals. *Class. Quantum Gravity* **33**, 184002 (2016).
33. Tanvir, N. R. et al. A ‘kilonova’ associated with the short-duration γ -ray burst GRB 130603B. *Nature* **500**, 547–549 (2013).
34. Just, O., Bauswein, A., Pulpillo, R. A., Goriely, S. & Janka, H.-T. Comprehensive nucleosynthesis analysis for ejecta of compact binary mergers. *Mon. Not. R. Astron. Soc.* **448**, 541–567 (2015).
35. Read, J. S. et al. Measuring the neutron star equation of state with gravitational wave observations. *Phys. Rev. D* **79**, 124033 (2009).
36. Lackey, B. D. & Wade, L. Reconstructing the neutron-star equation of state with gravitational-wave detectors from a realistic population of inspiralling binary neutron stars. *Phys. Rev. D* **91**, 043002 (2015).
37. Agathos, M. et al. Constraining the neutron star equation of state with gravitational wave signals from coalescing binary neutron stars. *Phys. Rev. D* **92**, 023012 (2015).
38. Abbott, B. P. et al. GW170817: measurements of neutron star radii and equation of state. *Phys. Rev. Lett.* **121**, 161101 (2018).
39. The LIGO Scientific Collaboration et al. A gravitational-wave standard siren measurement of the Hubble constant. *Nature* **551**, 85–88 (2017).
40. Hotokezaka, K. et al. A Hubble constant measurement from superluminal motion of the jet in GW170817. *Nat. Astron.* **3**, 940–944 (2019).
41. Planck Collaboration. Planck 2018 results. VI. Cosmological parameters. Preprint at <https://arxiv.org/abs/1807.06209> (2018).
42. Riess, A. G., Casertano, S., Yuan, W., Macri, L. M. & Scolnic, D. Large Magellanic Cloud Cepheid standards provide a 1% foundation for the determination of the Hubble constant and stronger evidence for physics beyond Λ CDM. *Astrophys. J.* **876**, 85 (2019).
43. Damour, T. & Deruelle, N. General relativistic celestial mechanics of binary systems. I. The post-Newtonian motion. *Ann. I.H.P. Phys. Theor.* **43**, 107–132 (1985).
44. Damour, T. & Deruelle, N. General relativistic celestial mechanics of binary systems. II. The post-Newtonian timing formula. *Ann. I.H.P. Phys. Theor.* **44**, 263–292 (1986).
45. Damour, T. & Taylor, J. H. Strong-field tests of relativistic gravity and binary pulsars. *Phys. Rev. D* **45**, 1840–1868 (1992).
46. Yao, J. M., Manchester, R. N. & Wang, N. A new electron-density model for estimation of pulsar and FRB distances. *Astrophys. J.* **835**, 29 (2017).
47. Lorimer, D. R. & Kramer, M. *Handbook of Pulsar Astronomy* Vol. 4 (Cambridge Univ. Press, 2004).

Publisher's note Springer Nature remains neutral with regard to jurisdictional claims in published maps and institutional affiliations.

© The Author(s), under exclusive licence to Springer Nature Limited 2020

Methods

Timing analysis

PSR J1913+1102 was discovered in 2012 by Einstein@Home in data from the PALFA survey⁷, which uses the William E. Gordon 305-m radio telescope at the Arecibo Observatory in Puerto Rico to search for pulsars within 5° of the Galactic plane. Since the discovery, we have been using the Arecibo Observatory to regularly monitor this pulsar with the Mock Spectrometer and the PUPPI pulsar backend system. This has been done as both a dedicated follow-up campaign for PSR J1913+1102 and regularly as a test source before PALFA observing sessions.

The times of arrival of these pulses were measured by cross-correlating each pulse profile with a noise-free representative template profile, from which we calculated a phase shift and apply it to the observed time stamp of the data profile⁴⁸. The uncertainty in each resulting pulse arrival time was determined by adopting the error in the calculated phase shift from the aforementioned correlation procedure. This process was carried out using the PSRCHIVE suite of analysis tools⁴⁹. Corrections between terrestrial time and the observatory clock were applied using data from Global Positioning System satellites and the Bureau International des Poids et Mesures. Our model also included input from the Jet Propulsion Laboratory DE436 Solar System ephemeris, in order to convert measured arrival times to the reference frame of the Solar System barycentre, by taking into account the motion of Earth.

These barycentred times of arrival were then compared to a predictive model of their expected arrival at Earth using the TEMPO pulsar timing software package (<https://github.com/nanograv/tempo>). Every rotation of the neutron star was enumerated relative to a reference observing epoch by accounting in our model for intrinsic pulsar properties, such as the rotation frequency and its spin-down rate, as well as its sky position and proper motion. We also addressed potential arrival-time delays due to the frequency-dependent refractive effect of the ionized interstellar medium by including the dispersion measure (DM) in our timing model, which is the integrated column density of free electrons along the line of sight between Earth and the pulsar. The relatively large value $DM = 339.026 \pm 0.005 \text{ pc cm}^{-3}$ for this pulsar explains why initial observations, primarily taken at an observing frequency centred at 1.4 GHz, displayed evidence of interstellar scattering that resulted in considerable smearing of the observed pulse shape due to multi-path propagation of the signal on its way to Earth⁷. This led to increased systematic uncertainties in the derived pulsar parameters, and we therefore switched to observations with the higher-frequency S-band Low receiver (centred at 2.4 GHz with a bandwidth of 800 MHz) to reduce these effects.

Along with these model parameters, our timing data resulted in an important measurement of the Keplerian orbital elements of the PSR J1913+1102 system, as well as several post-Keplerian parameters (these are quoted with 68% confidence-level uncertainties in Table 1). The latter are a theory-independent set of parameters that characterize perturbations on the Keplerian description of the orbit in the relativistic regime^{43–45}. As described in the main text, we have now improved the measurement precision of the orbital precession rate and determined the Einstein delay. From this, we were able to constrain the individual masses of the neutron stars in this system by assuming that general relativity is the correct theory of gravity, as encapsulated in the DDGR timing model^{43,44}. We have also made a precise determination of the orbital decay rate due to the emission of gravitational waves, which serve to remove orbital energy from the system over time. We expect the precision of the orbital decay to improve rapidly over time t (scaling as $t^{5/2}$) with further observations. It should also be noted that sources of kinematic biases can be introduced into the measured orbital decay and pulsar spin-down rates from apparent acceleration of the pulsar due to its tangential motion (that is, the Shklovskii effect⁵⁰) and the Galactic potential^{51,52}. We find the total proper motion of this pulsar to be $9.3 \pm 0.9 \text{ mas yr}^{-1}$, within 3σ of what would be expected if the PSR

J1913+1102 system were in the local standard of rest (6.50 mas yr^{-1}); this assumes a distance of 7.14 kpc. This distance is estimated from the measured value of DM, using a model of the Galactic free-electron density distribution⁴⁶. The total kinematic bias to the observed orbital decay corresponds to approximately one-third of the uncertainty in the orbital decay measurement. We are therefore confident that our measurements are consistent with intrinsic parameter values for the pulsar at the current level of uncertainty.

Once we apply our model to the dataset, we produce post-fit timing residuals—the difference between the predicted and observed pulse arrival times (Fig. 3). The timing precision achieved by this fit to our pulse arrival time data is characterized by the root-mean-square (r.m.s.) of the post-fit timing residuals. Our analysis of the PSR J1913+1102 dataset resulted in r.m.s. residuals of $56.1 \mu\text{s}$, consistent with the typical measured uncertainty in the observed pulse arrival times. We achieved a reduced χ^2 (that is, χ^2 divided by the number of degrees of freedom) of 1.01 for our fit, reaffirming the success of our timing model in describing the system, and implying that the timing residuals can be well represented by white Gaussian noise, as can be seen in Fig. 3.

Population synthesis

Modelling of the merger event that caused GW170817 has mostly relied on a DNS population consisting of roughly equal-mass neutron stars. Although this may be the result of a binary system with pre-merger mass ratio $q \approx 1$, the discovery of PSR J1913+1102 highlights the need to consider the effects of an asymmetric DNS merger. We note here for completeness that it is possible that GW170817 was caused by a neutron star–black hole merger. However, the abnormally low mass of the black hole in such a progenitor system would make this an unlikely scenario⁵³.

Previous studies^{54–57} simulated the population of DNS binaries from the measured parameters of known systems within a modelled Galactic pulsar population; this was done using the known sensitivities of the pulsar survey in which they were discovered. The modelling must account for selection effects, including the search degradation factor due to orbital acceleration, calculated from a semi-analytical model with the pulsar and companion masses and the system inclination as input⁵⁸. We calculated the probability density of the population of PSR J1913+1102-like DNSs that are beamed towards Earth ($N_{\text{obs}, J1913}$) using the more precisely measured orbital properties presented in this work. Assuming a beaming correction fraction for the pulsar⁵⁶ of $f_b = 4.6$, we derived the probability density of the total population ($N_{\text{tot}, J1913}$) of J1913+1102-like DNS systems in the Galaxy: ($N_{\text{pop}, J1913} = N_{\text{obs}, J1913} \times f_b$). The mode of the resulting distribution is $N_{\text{tot}, J1913} = 700_{-400}^{+2,600}$, where the uncertainties represent the 90% confidence interval of the distribution. This is consistent with previous estimates⁵⁶, but has smaller error bars owing to the updated orbital parameters and the addition of a new radio pulsar survey⁵⁷.

Owing to its small orbital period, the PSR J1913+1102 system will merge in 470 Myr, well within one Hubble time. There are eight other known DNS systems in the Galaxy that will also merge within the age of the Universe (which we henceforth refer to as merging DNSs, MDNSs). We obtained the individual probability densities of the population of these MDNSs using results given in previous studies^{56,57}. Assuming that these individual population distributions represent independent continuous random variables, we estimate the total population of MDNS systems in the Galaxy by convolving the individual population probability distributions, resulting in a mode $N_{\text{tot}, \text{MDNS}} = (11.4_{-3.8}^{+6.3}) \times 10^3$. Using our derived probability densities of PSR J1913+1102-like systems together with those of all MDNS systems, we then compute the probability density of PSR J1913+1102-like DNS systems in the Galaxy as a fraction of the MDNS population to be $11_{-9}^{+21} \%$ (90% confidence), using the median as the quoted value (with the mode of the distribution occurring at 6%); Fig. 2 presents the corresponding probability distribution. This in turn leads to an estimate that roughly one-tenth of detected DNS mergers result from the coalescence of an asymmetric binary system.

Data availability

All data are available from the corresponding author on request.

Code availability

The code used in this analysis is publicly available at: <https://github.com/nanograv/tempo> (pulsar timing analysis); <https://github.com/NihanPol/2018-DNS-merger-rate> (population synthesis); <https://github.com/rferdman/pypsr> (plotting tools).

48. Taylor, J. H. Pulsar timing and relativistic gravity. *Phil. Trans. R. Soc. A* **341**, 117–134 (1992).
49. Hotan, A. W., van Straten, W. & Manchester, R. N. PSRCHECK and PSRFITS: an open approach to radio pulsar data storage and analysis. *Publ. Astron. Soc. Pacif.* **21**, 302–309 (2004).
50. Shklovskii, I. S. Possible causes of the secular increase in pulsar periods. *Sov. Astron.* **13**, 562 (1970).
51. Nice, D. J. & Taylor, J. H. PSR J2019+2425 and PSR J2322+2057 and the proper motions of millisecond pulsars. *Astrophys. J.* **441**, 429–435 (1995).
52. Perera, B. B. P. et al. The dynamics of Galactic centre pulsars: constraining pulsar distances and intrinsic spin-down. *Mon. Not. R. Astron. Soc.* **487**, 1025–1039 (2019).
53. Kruckow, M. U., Tauris, T. M., Langer, N., Kramer, M. & Izzard, R. G. Progenitors of gravitational wave mergers: binary evolution with the stellar grid-based code COMBINE. *Mon. Not. R. Astron. Soc.* **481**, 1908–1949 (2018).
54. Kim, C., Kalogera, V. & Lorimer, D. R. The probability distribution of binary pulsar coalescence rates. I. Double neutron star systems in the Galactic field. *Astrophys. J.* **584**, 985–995 (2003).
55. Kim, C., Perera, B. B. P. & McLaughlin, M. A. Implications of PSR J0737-3039B for the Galactic NS-NS binary merger rate. *Mon. Not. R. Astron. Soc.* **448**, 928–938 (2015).
56. Pol, N., McLaughlin, M. & Lorimer, D. R. Future prospects for ground-based gravitational-wave detectors: the Galactic double neutron star merger rate revisited. *Astrophys. J.* **870**, 71 (2019); erratum 874, 186 (2019).

57. Pol, N., McLaughlin, M. & Lorimer, D. R. An updated Galactic double neutron star merger rate based on radio pulsar populations. *Res. Notes AAS* **4**, 22 (2020).
58. Bagchi, M., Lorimer, D. R. & Wolfe, S. On the detectability of eccentric binary pulsars. *Mon. Not. R. Astron. Soc.* **432**, 1303–1314 (2013).

Acknowledgements We thank S. Nisanke, T. Tauris and B. Metzger for constructive discussions, as well as C. Belczynski and T. Tauris for useful comments. The Arecibo Observatory is operated by the University of Central Florida, Ana G. Méndez-Universidad Metropolitana and Yang Enterprises under a cooperative agreement with the National Science Foundation (NSF; AST-1744119). R.D.F. and P.C.C.F. acknowledge the support of the PHAROS COST Action (CA16214). S.C., J.M.C., F. Crawford, M.A.M. and N.P. are members of the NANOGrav Physics Frontiers Center, which is supported by NSF award number PHY-1430284. S.C. and J.M.C. also acknowledge support from NSF award AAG-1815242. J.W.T.H. acknowledges funding from an NWO Vici grant ('AstroFlash'). V.M.K. acknowledges support from an NSERC Discovery Grant and Herzberg Award, the Canada Research Chairs programme, the Canadian Institute for Advanced Research and FRQ-NT. E.P. is a Vanier Canada Graduate Scholar. I.H.S. acknowledges support for pulsar research at the University of British Columbia by an NSERC Discovery Grant and by the Canadian Institute for Advanced Research. J.v.L. acknowledges funding from an NWO Vici grant ('ARGO').

Author contributions R.D.F. contributed to timing analysis, wrote and ran mass probability contour code, led proposals for observing campaigns for this pulsar with the Arecibo telescope, composed the manuscript and produced Figs. 1, 3. P.C.C.F. led the timing analysis. B.P.P.P. and N.P. led the population synthesis analysis and produced Fig. 2. R.D.F., P.C.C.F., B.P.P.P., F. Camilo, S.C., J.M.C., F. Crawford, J.W.T.H., V.M.K., M.A.M., E.P., I.H.S. and J.v.L. contributed to the PALFA survey operations, as well as the discovery and follow-up observations of this pulsar. All authors contributed to discussion regarding the content of this manuscript.

Competing interests The authors declare no competing interests.

Additional information

Correspondence and requests for materials should be addressed to R.D.F.

Peer review information Nature thanks Chris Belczynski and Thomas Tauris for their contribution to the peer review of this work.

Reprints and permissions information is available at <http://www.nature.com/reprints>.